Rare Metal Materials and Engineering
Volume
Available online at **www.rmme.ac.cn**

Cite this article as: Rare Metal Materials and Engineering,

DOI: 10.12442/j.issn.1002-185X.20240594

Relationship between Stress and Texture in L10-FePt Thin Films

Xuanli WANG [1], Wei LI [2*]

1. School of Materials and Metallurgy, Inner Mongolia University of Science and Technology, Baotou 014010 China; 2. Instrumental Analysis Center, Inner Mongolia University of Science and Technology, Baotou 014010 China

Abstract: $L1_0$-FePt thin film has been considered as a promising material for ultrahigh density perpendicular magnetic recording media. The texture type has a serious impact on the magnetic properties of $L1_0$-FePt thin films. In this study, the formation and evolution mechanisms of texture were discussed. The Reuss-Voigt-Hill models were used to determine the anisotropic elastic modulus of $L1_0$-FePt thin film with fiber texture. Then the strain energy of thin films under various stress conditions were caclucated. The results revealed the influence of stress condition on the fiber texture evolution. When the $L1_0$-FePt thin film was subjected to compressive in-plane strain prior to ordering transformation, the {100} fiber texture will be encouraged. On the contrary, the ordering transformation under tensile in-plane strain was promoted {001} fiber texture formation.

Key words: L10-FePt film; texture; stress; elastic modulus

In recent years, researchers have noticed that fiber texture in thin films are critical for the performance control of functional materials. Especially for L10-FePt thin film in perpendicular magnetic recording hard disks, due to the <001 > axis is the most easily magnetized axis, when L10-FePt thin film has strong {001} texture, it can exhibit excellent perpendicular magnetic anisotropy to meet the application requirements[1]. As a result, the research on fiber texture of L10-FePt thin film has attracted extensive attention. Many approaches have been tried to produce L10-FePt thin films with strong {001} fiber texture including: alternating deposition of Fe and Pt, employing a single crystal substrate, adding seed layer[2-5], magnetic field annealing and quick annealing[6,7], and adjusting film thickness[8-10]. How to enhance the {001} fiber texture in L10-FePt thin films has been the focus in most of the existing studies, yet lacking in-depth theoretical studies on the texture formation mechanism and texture control.

In thin films, the anisotropy of strain energy and surface energy is primary factor inducing the preferred growth of grains and the formation of fiber texture[11,12]. The elastic strain energy within thin films is intricately interconnected with their stress-strain and susceptible to modulation by external factors. These influences primarily from the residual strain present in as-deposited thin films, thermal strain resulting from disparities in thermal expansion coefficients between the film and substrate materials, and strain induced by the volumetric contraction of thin films due to defect annihilation and grain growth[13]. In addition to the aforementioned forms of strain, the strain caused by disorder-to-order phase transition exists in FePt thin films. FePt thin film is disordered FCC structure in as-deposited state, which is subjected to ordering transformation after annealing, thus forming ordered L10 phase with tetragonal structure. During the ordering transformation, the structure of FePt thin film changes, which gave rises to the change in lattice constant so as to generate a transformation strain. The stress state of FePt film will strongly affect grain growth orientation, and influence the formation of fiber texture.

Hence, the formation and evolution mechanisms of fiber texture in L10-FePt thin films were systematically explored

Received date:
Foundation item: Inner Mongolia Natural Science Foundation Project (2020LH05028)
Corresponding author: Li Wei, Ph.D., Professor, Instrumental Analysis Center, Inner Mongolia University of Science and Technology, Baotou, 014010, P. R. China, Tel: 0472-5288100, E-mail: liwei_imust@126.com

and discussed in this study. In detail, the anisotropic strain energy in L10-FePt thin films was calculated, and the influence of the changes in external stress on their fiber textures was analyzed, expecting to provide an effective reference for preparing L10-FePt thin films with strong {001} fiber textures.

1 Calculation Procedure

1.1 Anisotropic elastic modulus

Elastic modulus is anisotropic due to different interatomic binding forces in different crystal orientations[14]. The anisotropic strain energy in $L1_0$-FePt thin films could be accurately calculated only by calculating the elastic constant and elastic modulus of different crystal planes in the films.

Reuss, Voigt and Hill models have been employed to calculate the macro-elastic constant of polycrystals. Reuss model is a iso-stress model after averaging the elastic flexibility coefficients of all grains in different orientations. As for Voigt model (an iso-strain model), the elastic rigidity coefficients of all grains in different orientations are averaged. The elastic constants calculated by the above two models are the upper and lower limits of actual value, between which, however, the real value falls. Hill model expresses the elastic constant of a material by taking the arithmetic mean of the results calculated by the above two models[15].

Orientation distribution function (ODF), which describes the three-dimensional spatial distribution of textures, is mainly applied to analyze the textures of various polycrystalline materials at present. The elastic constant of anisotropic materials deviates, to a great extent, from that of isotropic materials. Given this, ODF could be used to calculate the elastic constant, denote the relationship between texture coefficient and elastic constant, quantitatively analyze the change in the elastic constant with the texture and further clarify the stress-texture relationship in the FePt thin film. As shown in Figure 1, the sample coordinate system Pi and crystal coordinate system Ki of a polycrystalline film were defined to describe the crystal orientations in polycrystals. As for the crystal coordinate system, a total of 3 mutually perpendicular crystal orientations were chosen according to the crystal symmetry. In general, the crystal coordinate system did not overlap with the sample coordinate system, and the included angle between the two was expressed by three Euler angles (φ_1, ϕ, φ_2).

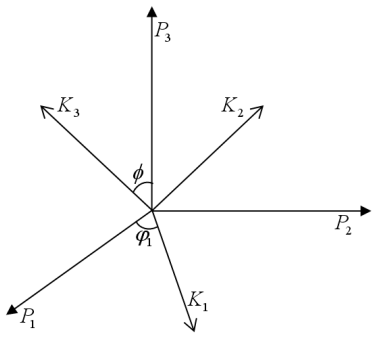

Figure.1 Schematic diagram of crystal and sample coordinate system of polycrystal

During calculation, the elastic constant needed to be transformed from the crystal coordinate system to the sample coordinate system via a transformation matrix, as follows:

$$C'_{ijkl}=a_{im}a_{jn}a_{ko}a_{lp}C_{mnop} \quad (1)$$

$$S'_{ijkl}=a_{im}a_{jn}a_{ko}a_{lp}S_{mnop} \quad (2)$$

Where C'_{ijkl} and S'_{ijkl} represent the elastic rigidity coefficient and elastic flexibility coefficient in the sample coordinate system, respectively. C_{mnop} and S_{mnop} stand for the monocrystal elastic rigidity coefficient and monocrystal elastic flexibility coefficient in the crystal coordinate system, respectively. a_{ij} (i, j=1,2,3) is a transformation matrix from the sample coordinate system to the crystal coordinate system. This transformation matrix was expressed by Euler angles to facilitate the integration of Euler space in statistical calculation.

$$a_{ij}=\begin{bmatrix} \cos\varphi_1\cos\varphi_2-\sin\varphi_1\sin\varphi_2\cos\phi & \sin\varphi_1\cos\varphi_2+\cos\varphi_1\sin\varphi_2\cos\phi & \sin\varphi_2\sin\phi \\ -\cos\varphi_1\sin\varphi_2-\sin\varphi_1\cos\varphi_2\cos\phi & -\sin\varphi_1\sin\varphi_2+\cos\varphi_1\cos\varphi_2\cos\phi & \cos\varphi_2\sin\phi \\ \sin\varphi_1\sin\phi & -\cos\varphi_1\sin\phi & \cos\phi \end{bmatrix} \quad (3)$$

Since the $L1_0$-FePt thin film has a tetragonal structure with a lattice constant of a=b≠c, the transformation matrix a_{ij} should be multiplied by a coefficient matrix T:

$$T=\begin{bmatrix} 1 & 0 & 0 \\ 0 & 1 & 0 \\ 0 & 0 & c/a \end{bmatrix} \quad (4)$$

1. Reuss model

Based on Reuss model, the average macro-elastic flexibility coefficient S'_{ijkl} of polycrystal materials should be the probability weighted average of monocrystal elastic flexibility coefficients (S_{mnop}) of all grains based on their spatial orientation distribution[16]. The macro-elastic constant could be solved by calculating the average value of elastic constants of all grains in their testing orientations:

$$\overline{S}^{R}_{ijkl}=\frac{1}{8\pi^2}\int_{\Omega}S'_{ijkl}\cdot f(g)dg=\frac{1}{8\pi^2}\int_0^{2\pi}\int_0^{\pi}\int_0^{2\pi}a_{im}a_{jn}a_{ko}a_{lp}S_{mnop}f(g)\sin\phi d\phi d\varphi_1 d\varphi_2 \quad (5)$$

Where f(g) denotes the normalized ODF, and Ω represents the orientation space of grains. The rigidity coefficient under Reuss model could be obtained by finding the inverse matrix of flexibility matrix:

$$\overline{C}^{R}_{ijkl}=\left[\overline{S}^{R}_{ijkl}\right]^{-1} \quad (6)$$

In case that the material possessed an ideal fiber texture, the above equation could be simplified as below:

$$\left\langle \overline{S}^{R}_{ijkl} \right\rangle^{hkl} = \frac{1}{2\pi}\int_0^{2\pi} S'_{ijkl} f(g) d\phi_1 \quad (7)$$

2. Voigt model

Similar to Reuss model, the average macro-elastic rigidity coefficient was obtained by solving the probability weighted average of monocrystal elastic rigidity coefficients of all grains in the crystal coordinate system according to their spatial orientation distribution. If the orientation correlation between adjacent grains, the grain shape and the intergranular interaction were ignored, the elastic constant could be expressed as follows:

$$\overline{C}^{V}_{ijkl} = \frac{1}{8\pi^2}\int_{\Omega}^{2\pi} C'_{ijkl} \cdot f(g) dg = \frac{1}{8\pi^2}\int_0^{2\pi}\int_0^{\pi}\int_0^{2\pi} a_{im}a_{jn}a_{ko}a_{lp}C_{mnop} f(g)\sin\phi d\phi d\phi d\varphi_1 d\varphi_2 \quad (8)$$

When the material was of an ideal fiber texture, one or two among the three Euler angles (φ_1, ϕ and φ_2) were fixed, and then the above equation was simplified into the following form:

$$\left\langle \overline{C}^{V}_{ijkl} \right\rangle^{hkl} = \frac{1}{2\pi}\int_0^{2\pi} C'_{ijkl} f(g) d\phi_1 \quad (9)$$

Then, the transformation matrix a_{ij} was substituted into Equations (7) and (9) to solve the elastic flexibility coefficient and elastic rigidity coefficient of this material under the corresponding coordinate systems in the case of an ideal fiber texture.

3. Hill model

Based on the results of Reuss and Voigt models, the arithmetic mean of macro-flexibility coefficient and rigidity coefficient of this material was solved as Hill approximate value:

$$\overline{S}^{H}_{ijkl}=\frac{1}{2}\left\{\overline{S}^{R}_{ijkl}+\left[\overline{C}^{V}_{ijkl}\right]^{-1}\right\};\ \overline{C}^{H}_{ijkl}=\frac{1}{2}\left\{\overline{C}^{R}_{ijkl}+\left[\overline{S}^{V}_{ijkl}\right]^{-1}\right\}; \quad (10)$$

The expression of Hooke's law is as below:

$$\sigma_{ij} = C_{ijkl}\varepsilon_{kl},\quad \varepsilon_{ij} = S_{ijkl}\sigma_{kl} \quad (11)$$

Where C_{ijkl} is the elastic rigidity coefficient, which manifests the relationship between two second-order tensors, namely, stress σ and strain ε, generated inside the material under stress conditions. S_{ijkl} stands for the elastic flexibility coefficient. The two matrices were mutually reversible to an appropriate extent, i.e: $S_{ijkl}=[C_{ijkl}]^{-1}$.

After the subscripts of coefficients were simplified, the above Hooke's law could be written into $\sigma_q = C_{qr}\varepsilon_r$ and $\varepsilon_q = S_{qr}\sigma_r$ (q, r=1, 2, 3, 4, 5, 6). The monocrystal elastic rigidity coefficient was assumed as C_{qr}, and then C'_{qr} corresponding to any orientation(φ_1, ϕ and φ_2) could be obtained through the transformational relation of tensors. Next, the double-subscript matrix component of the rigidity coefficient was reduced into a four-subscript tensor component and then substituted into the coordination conversion formula of tensors as below:

$$C'_{qr}=C'_{ijkl}=a_{im}a_{jn}a_{ko}a_{lp}C_{mnop} \quad (12)$$

$$S'_{qr}=S'_{ijkl}=a_{im}a_{jn}a_{ko}a_{lp}S_{mnop} \quad (13)$$

The elastic constants of monocrystal $L1_0$-FePt materials are listed in Table 1[17]. On this basis, the elastic constants of isotropic $L1_0$-FePt materials under Reuss, Voigt and Hill models could be solved (Table 2).

Table 1: Elastic constants of monocrystal L10-FePt materials (Cij/Gpa，Sij×10-3/ Gpa)

	C_{11}	C_{12}	C_{13}	C_{33}	C_{44}	C_{66}
$L1_0$-FePt	261	169	151	299	103	133
	S_{11}	S_{12}	S_{13}	S_{33}	S_{44}	S_{66}
	0.007237	-0.00363	-0.00182	0.005183	0.009709	0.007519

Table 2: Elastic constants of isotropic L10-FePt materials (Cij/Gpa)

Model	C_{11}	C_{12}	C_{13}	C_{33}	C_{44}	C_{66}
Voigt	249	169	161	226	65	68

Reuss	247	165	156	219	67	66
Hill	248.4	167	158.5	222.5	66	67

When a fiber structure was generated in the $L1_0$-FePt thin film, the Miller index (hkl) of crystal face could be determined to express three Euler angles (φ_1, ϕ, φ_2):

$$\phi=\arccos\frac{l}{\sqrt{h^2+k^2+l^2}},\quad \varphi_1=\arcsin\left[\frac{w}{\sqrt{u^2+v^2+w^2}}\cdot\sqrt{\frac{h^2+k^2+l^2}{h^2+k^2}}\right],$$

$$\varphi_2=\arccos\frac{k}{\sqrt{h^2+k^2}}$$

If the $L1_0$-FePt thin film had the following ideal fiber textures, its Miller index was substituted into Formulas (7), (9) and (10) to acquire the following results (Table 3).

When the thin film material was isotropic, its biaxial elastic modulus was correlated with Young's modulus and Poisson's ratio. However, the effect of anisotropy must be taken into account when fiber textures existed in the thin film, that is, grains grew along a specific orientation or a specific crystal face in grains was parallel to the surface of the thin film. Under the sample coordinate system, the biaxial elastic modulus M of the thin film could be expressed as below[18]:

$$M=C_{11}+C_{12}-\frac{2C_{13}^2}{C_{33}} \tag{14}$$

Where the C coefficient could be transformed into the following expression through Equation (13):

$$M^V=[c_{11}^F]+[c_{12}^F]-\frac{2[c_{13}^F]^2}{[c_{33}^F]} \tag{15}$$

Where:

$[c_{11}^F]+[c_{12}^F]=c_{11}+c_{12}-c_0^T\Gamma_{hkl}^T+2Z(c_1^TZ+2\Delta c_{12}+2\Delta c_{66})+2c_{16}Z_1$

$[c_{13}^F]=c_{13}+c_0^T\Gamma_{hkl}^T+Z\{c_1^T(1-2Z)-\Delta c_{12}\}-2c_{16}Z_1$

$[c_{33}^F]=c_{33}-2c_0^T\Gamma_{hkl}^T-4Z\{c_1^T(1-Z)+\Delta c_{12}+2\Delta c_{66}\}+4c_{16}Z_1$

$c_0^T=c_{11}-c_{12}-2c_{66}$, $c_1^T=\Delta c_{11}-2\Delta c_{12}-4\Delta c_{66}$,

$\Delta c_{11}=c_{33}-c_{11}$, $\Delta c_{12}=c_{13}-c_{12}$, $\Delta c_{66}=c_{44}-c_{66}$

$$Z=\frac{(h^2+k^2)}{2\left[h^2+k^2+(la/c)^2\right]^2},\quad Z_1=\frac{hk(h^2-k^2)}{\left[h^2+k^2+(la/c)^2\right]^2},\quad \Gamma_{hkl}^T=\frac{h^2k^2+(h^2+k^2)(la/c)^2}{\left[h^2+k^2+(la/c)^2\right]^2}$$

According to the above formula, the elastic modulus of $L1_0$-FePt film with ideal fiber texture can be obtained, as shown in Table 4. According to the calculation results, $L1_0$-FePt thin films presented evidently different elastic properties under different types of textures, indicating that the elastic moduli of $L1_0$-FePt thin films is intensely impacted by the texture.

Table 3: Elastic constants of L10-FePt materials with (hkl) fiber textures (Cij/Gpa)

（hkl）	Model	C_{11}	C_{12}	C_{13}	C_{33}	C_{44}	C_{66}
(001)	Voigt	254.6	175.4	152.8	297	89.1	72.9
	Reuss	252	174.8	150.6	305	86.5	69.8
	Hill	253.3	175.1	151.7	298	87.8	71.5
(110)	Voigt	255.8	194.3	136.2	318.5	92.5	69.3
	Reuss	254.3	186.3	132.2	314.1	90.4	65.2
	Hill	255.5	190.6	134.2	316.3	91.5	67.3
(111)	Voigt	263.6	208.3	111.1	374.5	76.8	66.5
	Reuss	261.4	203.5	107.4	370.1	74.8	63.8
	Hill	262.5	205.9	109.5	372.3	75.8	65.3
(100)	Voigt	260.6	170.4	160	261	74.2	70.9
	Reuss	257.7	167.3	158.6	257.5	72.6	67.4
	Hill	259.15	168.6	159.3	259.3	73.3	69.2
(011)	Voigt	257.1	199.3	126.9	342.9	75.1	67
	Reuss	255.4	195.6	123.2	339.7	73.3	63.4
	Hill	256.3	197.5	124.6	341.3	74.2	65.2

Table 4: Elastic properties of $L1_0$-FePt materials with (hkl) fiber texture

Texture	Young's modulus E(GPa)	biaxial elastic modulus M(GPa)	Poisson's ratio ν
(001)	241.43	277.48	0.355
(110)	253.87	333.17	0.373
(111)	216.83	406.05	0.411
(100)	201.48	234.83	0.357
(011)	210.89	362.23	0.403

1.2 Elastic strain energy of $L1_0$-FePt thin films

$L1_0$-FePt thin film will be impacted by external stress and transformation stress during growth, and the change in stress state influences the strain energy in the thin film and finally leads to the formation of various fiber texture. Therefore, calculating the strain energy of $L1_0$-FePt films under different stress states and discussing the relationship between stress and texture are the key to clarify the mechanism of texture formation.

In this study, the thickness of $L1_0$-FePt thin film is much smaller than substrate thickness, and the external stress posing to it was completely reflected by the binding force of the substrate against the thin film, and thus it was subjected to an equivalent biaxial stress so as to generate the in-plane biaxial strain. In this case, the in-plane strain of $L1_0$-FePt thin film is assumed to be a variation range from compressive strain to tensile strain. On this basis, the strain energy of $L1_0$-FePt thin film is discussed.

For polycrystalline films with fiber texture, the orientation of out-plane grains are consistent, but in-plane grains show randomly distributed orientation. Under the in-plane equivalent biaxial stress, all in-plane grains generate the same strain. For the sake of simplicity, all grains in the $L1_0$--FePt thin film were regarded as isometric crystals, and the in-plane strain could be denoted by the circumcircle radius of the crystal face, so as to calculate the strain generated by the thin film as shown in Figure 4 (a). In addition, the [001] crystal orientation was designated as the c axis after ordering phase transition, Figure 4 (b) is the crystal coordinate system of $L1_0$-FePt. In the Figure 4 (c), the grains in all orientations within the $L1_0$-FePt thin film before ordering transformation were considered as the circumcircle with a radius of R and those after ordering transformation as the circumcircle with a radius of R'. In this way, the strain generated by external stress and that by ordering transformation were effectively associated to accurately calculate the strain energy of the $L1_0$-FePt thin film.

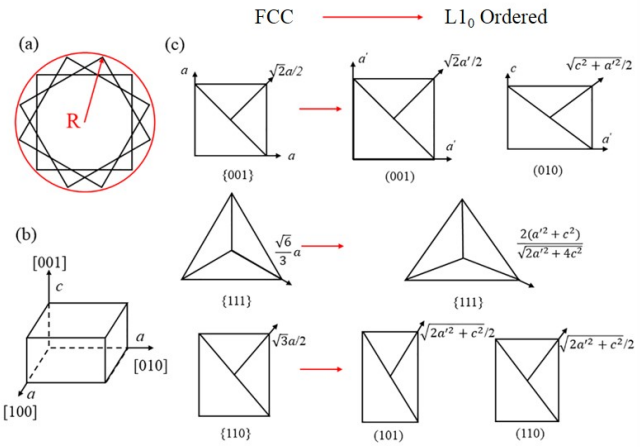

Figure 4: In-plane strain of the thin film: (a) Unit volume circle; (b) Crystal coordinate system of $L1_0$-FePt; (c) Change in the radius of unit volume circle before and after ordering transformation of crystal faces in different orientations

The strain energy of the $L1_0$-FePt thin film under ideal textures of {001}, {010}, {111}, {101} and {110} were mainly calculated. It could be observed from Figure 4 (c) that in the case of ordering transformation, different transformation strains were generated on the crystal faces of different orientations, which could be expressed by the radius difference of the unit volume circle before and after ordering transformation:

$$\varepsilon_t = \left(\frac{R'-R}{R}\right) \tag{16}$$

The in-plane strain generated by external stress in the thin film before ordering transformation could be denoted by the coefficient k. The range of in-plane strain generated by the external environment to the $L1_0$-FePt thin film was assumed to be (-3% – +3%), and the thin film experienced ordering transformation under different external stresses.

The elastic strain energy of $L1_0$-FePt thin films with different fiber textures could be denoted as follows:

$$W_{hkl}=M_{hkl}\left(\frac{R'-R(1+k)}{R(1+k)}\right)^2 \quad (17)$$

2 Results and discussion

According to the anisotropic elastic modulus of $L1_0$-FePt film, the elastic strain energy of $L1_0$-FePt film under the combined action of external stress and phase change stress is obtained. The results are shown in Figure 5. The differently colored curves represent the strain energies under different types of textures. The calculation results showed that the strain energy of $L1_0$-FePt thin films with different fiber textures is substantially influenced by the in-plane strain state.

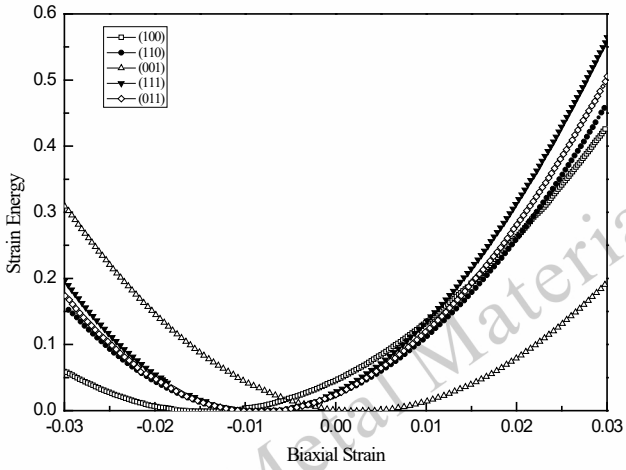

Figure 5. Change curves of strain energy in $L1_0$-FePt thin films under different in-plane strain states

When ordering transformation occurred to the $L1_0$-FePt thin film, 0–0.5% of in-plane compressive strain existed, different types of fiber textures varied not obviously in the elastic strain energy, and the surface energy of the thin film was the main driving force for forming textures. As the in-plane compressive strain started rising from 0.5%, the difference between different fiber textures in strain energy was initially enlarged, and the {100} plane in the thin film reached the minimum strain energy while the {001} plane showed the maximum strain energy. With the further increase in the in-plane compressive strain, an increasingly evident difference of strain energy was observed between {100} and {001} plane. The formation of {100} fiber textures in the $L1_0$-FePt thin film was facilitated by minimizing the strain energy if the thin film was subjected to ordering transformation under a large in-plane compressive strain. However, when it was under an in-plane tensile strain state, the {001} crystal face reached the minimum strain energy, and the difference of this crystal face from other crystal faces was more and obvious with the increase in the in-plane tensile strain, thus promoting the formation of {001} fiber textures in the $L1_0$-FePt thin film.

Hence, in order to obtain $L1_0$-FePt films with strong {001} fiber texture, FePt films are placed in the in-plane tensile stress state before the ordering transformation. Moreover, the larger the in-plane tensile strain, the more conducive to the formation of {001} fiber.

3 Conclusion

In this study, the influence of stress on the variant selection for $L1_0$-FePt thin films during ordering transformation was explored. Subsequently, the anisotropic elastic moduli of $L1_0$-FePt thin films and their anisotropic elastic strain energies under different stress states were theoretically calculated. On this basis, the stress-texture interactive relationship in $L1_0$-FePt thin films was established. When $L1_0$-FePt thin film is under in-plane compressive stress state during ordering transformation, the formation of {100} fiber textures will be promoted. On the contrary, {001} fiber textures tend to appear when it is under a tensile stress state. Moreover, a greater in-plane tensile stress borne by the $L1_0$-FePt thin film during ordering transformation will contribute to stronger {001} fiber textures.

Acknowledgements

The authors would like to acknowledge financial support by the Inner Mongolia Natural Science Foundation Project (2020LH05028).

References

[1] Zhang L, Takahashi Y K, Perumal A, et al. $L1_0$-ordered high coercivity (FePt)Ag-C granular thin films for perpendicular recording [J]. Journal of Magnetism and

Magnetic Materials, 2010, 322(18): 2658-2664.

[2] Kang K, Zhang Z G, Papusoi C, et al. Composite nanogranular films of FePt-MgO with (001) orientation onto glass substrates [J]. Applied Physics Letters, 2004, 84(3): 404-406.

[3] Weisheit, M. Textured growth of highly coercive $L1_0$ ordered FePt thin films on single crystalline and amorphous substrates [J]. Journal of Applied Physics, 2004, 95(11): 7489-7491.

[4] Hotta A, Ono T, Hatayama M, et al. Magnetic anisotropy and order structure of $L1_0$-FePt(001) single-crystal films grown epitaxially on (001) planes of MgO, $SrTiO_3$, and $MgAl_2O_4$ substrates [J]. Journal of Applied Physics, 2014, 115(17): 17B712.

[5] Shima T, Moriguchi T, Mitani S, et al. Low-temperature fabrication of $L1_0$ ordered FePt alloy by alternate monatomic layer deposition [J]. Applied Physics Letters, 2002, 80(2): 288-290.

[6] Liu L, Hua L, Wei S, et al. Orientation control in $L1_0$ FePt films by using magnetic field annealing around Curie temperature [J]. Applied Surface Science, 2012, 258(15): 5770-5773.

[7] Ishio S, Narisawa T, Takahashi S, et al. L10 FePt thin films with [001] crystalline growth fabricated by SiO_2 addition - Rapid thermal annealing and dot patterning of the films [J]. Journal of Magnetism & Magnetic Materials, 2012, 324(3): 295-302.

[8] Dang H, Liu L, Hao L, et al. Orientation-controlled nonepitaxial $L1_0$ FePt thin films [J]. Journal of Applied Physics, 2014, 115(17): 17B711.

[9] Mei J K, Yuan F T, Liao W M, et al. Critical Thickness of (001) Texture Induction in FePt Thin Films on Glass Substrates [J]. IEEE Transactions on Magnetics, 2011, 47(10): 3633-3636.

[10] Sun A C, Hsu J H, Kuo P C, et al. Thickness limit in perpendicular magnetic anisotropy $L1_0$ FePt (001) thin film [J]. Journal of Magnetism & Magnetic Materials, 2007, 310(2): 2650-2652.

[11] Thompson C V, Carel R. Texture development in polycrystalline thin films [J]. Materials Science & Engineering B, 1995, 32(3): 211-219.

[12] Ellis E A, Chmielus M, Lin M T, et al. Driving forces for texture transformation in thin Ag films [J]. Acta materialia, 2016, 61(19): 7121-7132.

[13] Zeiger W, Brückner W, Schumann J, et al. Stress development in $FeAl_8$ thin films during heat treatment [J]. Thin Solid Films, 2000, 370(1-2): 315-320.

[14] Welzel, U., Fréour S, Mittemeijer E J. Direction-dependent elastic grain-interaction models-a comparative study [J]. Philosophical Magazine, 2005, 85(21): 2391-2414.

[15] Noyan I C, Cohen J B. Residual stress: measurement by diffraction and interpretation [M]. Residual Stress: Measurement by Diffraction and Interpretation, 1987.

[16] Bunge, Joachim H. Texture-The Key to Physics in Polycrystalline Matter [J]. Materials Science Forum, 1998, 273-275(0): 3-14.

[17] Müller M, Erhart P, Albe K. Thermodynamics of $L1_0$ ordering in FePt nanoparticles studied by Monte Carlo simulations based on an analytic bond-order potential [J]. Physical Review B, 2007,76(15): 155412

[18] Feng H, Weaver M L. Effective biaxial modulus of ideally (hkl)-fiber-textured hexagonal, tetragonal, and orthorhombic films [J]. Journal of Applied Physics, 2006, 100(9): 093523.

[19] Mei J K, Yuan F T, Liao W M, et al. Effect of initial stress/strain state on formation of (001) preferred orientation in $L1_0$ FePt thin films [J]. Journal of Applied Physics, 2011, 109(7): 07A737.

$L1_0$-FePt 薄膜应力与织构的关系

王炫力[1]，李玮[2]

(1 内蒙古科技大学 材料科学与工程学院 内蒙古 包头 0140101

2 内蒙古科技大学 分析测试中心 内蒙古 包头 014010；)

摘 要：L10-FePt 薄膜是一种有前景的超高密度垂直磁记录介质材料。织构类型对 L10-FePt 薄膜的磁性能有强烈的影响。本研究探讨了织构的形成和演化机制。用 Reuss-Voigt-Hill 模型确定了具有纤维织构 L10-FePt 薄膜的各向异性弹性模量。然后计算了薄膜在不同应力条件下的弹性应变能。研究结果揭示了应力条件对纤维织构演变的影响。当 L10-FePt 薄膜在有序转变之前受到平面压缩应力时，(100)纤维织构将得到促进。相反，平面拉伸应变下的有序转变促进了 (001)纤维织构的形成。

关键词：L10-FePt薄膜; 织构; 应力; 弹性模量

作者简介：李玮，男，1988 年生，博士，副教授，内蒙古科技大学 ，内蒙古 包头 014010，电话：0472-5288100，E-mail: liwei_imust@126.com